Inorganic Chemistry
Cite This: Inorg. Chem. XXXX, XXX, XXX–XXX
Article
pubs.acs.org/IC

# A Thiophene-2-carboxamide-Functionalized Zr(IV) Organic Framework as a Prolific and Recyclable Heterogeneous Catalyst for Regioselective Ring Opening of Epoxides

Aniruddha Das,[†] Nagaraj Anbu,[‡] Helge Reinsch,[§] Amarajothi Dhakshinamoorthy,*[,‡] and Shyam Biswas*[,†]

[†]Department of Chemistry, Indian Institute of Technology Guwahati, Guwahati, Assam 781039, India
[‡]School of Chemistry, Madurai Kamaraj University, Madurai, Tamil Nadu 625021, India
[§]Institut für Anorganische Chemie, Christian-Albrechts-Universität, Max-Eyth-Strasse 2, 24118 Kiel, Germany

Supporting Information

**ABSTRACT:** A new thiophene-2-carboxamide-functionalized Zr-UiO-66 MOF (**1**) was synthesized by employing a traditional solvothermal procedure. Compound **1** displayed high thermal (up to 340 °C under an Ar atmosphere) and chemical stability (in water, 1 M HCl, and acetic acid). A nitrogen physisorption measurement with the activated form of **1** (denoted **1′**) exhibited a BET surface area (781 $m^2/g$) despite attachment of a bulky side chain with the linker molecule. Compound **1′** was able to heterogeneously catalyze the ring-opening reaction of epoxides with amines. Catalyst **1′** exhibited significant yields as well as wide substrate scope in the ring opening of epoxides by means of amines. It also displayed better catalytic performance in comparison to known MOF catalysts such as $Cu_3(BTC)_2$, Fe(BTC) (BTC: 1, 3, 5-benzenetricarboxylate), and Zr-UiO-66. Control experiments were performed with free linker, Zr(IV) salt and without catalyst **1′**, confirming the exclusive role of **1′** in the catalytic reaction. The reusability characteristics of catalyst **1′** was established for up to five consecutive catalytic cycles. The synthesis and characterization of the linker molecule, material **1**, and **1′** and mechanism of the catalysis reaction were studied elaborately.

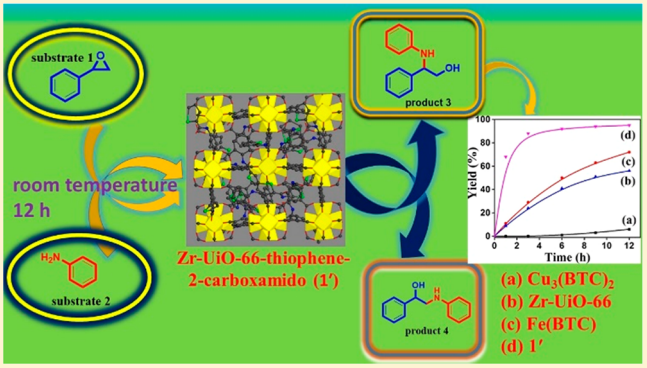


## INTRODUCTION

Epoxides are considered to be privileged molecules in organic chemistry because of their versatile nucleophilic opening character, producing 1,2-difunctionalized structures, and also because such cleavages often occur with trans stereochemistry.[1−4] In the field of asymmetric catalysis, β-amino alcohols are significant as chiral ligands and chiral auxiliaries mostly originating from nature.[5−9] Amino alcohols are often derivatized to increase their chelating abilities or steric influences.[10,11] In the fields of synthetic organic chemistry, biological chemistry, and medicinal industry, β-amino alcohols have occupied a dominant position because they are used as building units for therapeutic agents, insecticidal agents, β-blockers, antimalarial agents, and numerous biologically active natural products.[12−17] Cyclic amino alcohols such as quinines are a class of naturally occurring, biologically active products that are required in the treatment of malaria.[18] Renin and HIV-1 protein inhibitors constitute pharmacologically active amino alcohols, and one such example is saquinavir.[18] Often, β-adrenergic blockers, which constitute a class of β-amino alcohols, are used to regulate cardiovascular diseases such as hypertension, cardiac arrhythmias, and angina pectoris.[18−21]

Ring opening of oxiranes by nucleophilic attack of various amines is the easiest way to prepare β-amino alcohols.[7,22] However, this approach is not acceptable due to its disadvantages such as the sluggish reaction rate because of the sensitivity of epoxides and decrease in regioselectivity. There are many reports involving the preparation of β-amino alcohols utilizing epoxides as electrophiles.[17,23−29] Researchers have designed several routes such as the use of homogeneous catalysts,[30,31] alumina,[1] alkali metals,[32] metal amides,[33] and silica gel in order to increase the electrophilicity of epoxides. Unfortunately, most of these methods have several drawbacks such as the moisture-sensitive character of the catalysts, the low efficiency of catalysts, long reaction time, less regioselectivity, high reaction temperature and pressure, poor yield and recyclability, etc.[1,4,22,34−36]

Three-dimensional (3D) metal-organic frameworks (MOFs) , being stable, very crystalline solid porous compounds, have attracted much scientific interest for gas adsorption and separation,[37−39] heterogeneous catalysis of

Received: August 30, 2019






DOI: 10.1021/acs.inorgchem.9b02608
Inorg. Chem. XXXX, XXX, XXX–XXX

numerous organic reactions,[40−43] sensing,[44−47] photonic applications,[46] drug delivery,[48] proton conductivity,[49] etc. Moreover, porous MOFs have shown considerable heterogeneous catalytic activities in many organic reactions because of their insoluble character, exceptionally large surface area,[40] tunable pore size,[50] adjustable internal surface properties, and easy separation of the catalyst after reaction.[51] In this regard, Zr-MOFs possessing exceptional thermal as well as high chemical stabilities are considered as remarkable candidates for various heterogeneous catalysis reactions.[34,52−57] Synthetically, new MOFs with desirable structures and specific properties can be designed and synthesized by tuning the side functional groups of linker molecules. In case of epoxide ring-opening reactions by means of amines, those catalysts are preferred, which enhance the electrophilic character of epoxides or increase the nucleophilic character of amines.

Keeping in mind all the factors mentioned above, we have designed a new Zr(IV)-based UiO-66 compound having a thiophene-2-carboxamide side functional moiety attached with the linker molecule. We have explored the heterogeneous catalytic activity of this compound in the ring-opening reactions of epoxides by amines. The Zr-UiO-66 compound with a thiophene-2-carboxamido functionality was synthesized solvothermally and systematically characterized. The compound showed thermal stability and chemical stability toward water and acids (acetic acid and 1 M HCl). Compound **1′** can be considered as a porous material due to its large BET surface area (781 $m^2/g$). The catalytic performances of **1′** are outstanding in terms of remarkable yield, purity and regioselecivity of products, size selectivity of substrates, and reusability of the catalyst.

## EXPERIMENTAL SECTION

**Synthesis of $[Zr_6O_4(OH)_4(BDC\text{-}C_5H_4NOS)_6]\cdot 4.5H_2O\cdot 3.5DMF$ (Zr-UiO-66-thiophene-2-carboxamido, 1).** $ZrCl_4$ (32 mg, 0.14 mmol) and 2-(thiophene-2-carboxamido)benzene-1,4-dicarboxylic acid linker ($H_2BDC\text{-}C_5H_4NOS$; 40 mg, 0.14 mmol) were placed in a glass tube in a 1:1 molar ratio. *N,N*-Dimethylformamide (DMF; 2 mL) and formic acid (572 $\mu$L, 4.55 mmol) were poured into the glass tube holding the reaction mixture. Afterward, the glass tube was placed onto a block heater which was maintained at 120 °C for 1 day. After 1 day, a white precipitate was collected by vacuum filtration, followed by washing with acetone. For drying purposes, the powder sample was kept inside an oven at 80 °C for 4 h. The yield calculated considering the zirconium salt was 58 mg (0.02 mmol, 92%). Anal. Calcd for $C_{88.5}H_{85.5}N_{9.5}O_{46}S_6Zr_6$ (2757.90 g $mol^{-1}$): C, 38.54; H, 3.12; N, 4.82. Found: C, 38.41; H, 2.63; N, 4.73%. FT-IR (KBr, $cm^{-1}$): 3436 (br), 1646 (s), 1582 (s), 1509 (w), 1423 (vs), 1380 (vs), 1306 (s), 1258 (s), 1170 (w), 1110 (w), 1070 (w), 858 (w), 767 (vs), 738 (w), 662 (vs), 596 (w), 542 (w), 481 (s).

**Activation of Compound 1.** Activation of compound **1** was carried out in two stages. In the first stage, 100 mg of compound **1** was dispersed in methanol (25 mL) and stirring was conducted at room temperature for 1 day. Later, the solvent was removed by filtration and drying of the precipitate was executed inside an oven at 70 °C for 4 h. Finally, the solid powder was placed in a sealed activation tube, which was degassed for 1 day at 130 °C to achieve the activated sample, denoted **1′**.

**Reaction Procedure.** In a typical reaction, substrate **1** (0.6 mmol) and substrate **2** (0.5 mmol) were placed in a reaction vessel containing 15 mg of catalyst. Then, this mixture was mixed thoroughly and kept for 12 h under ambient conditions. The progress of the ring opening of epoxide reaction with respect to time was monitored by gas chromatography (GC) through sampling of aliquots at various time intervals. GC was utilized to access the yield of the final product by means of internal standard method. Identification of the products was carried out by using GC-MS and $^1H$ NMR techniques (Figures S12−S49 in the Supporting Information). At the end of the reaction, diluting of the mixture, washing the catalyst with dichloromethane (2 × 5 mL), and drying (at 80 °C for 45 min) were carried out consecutively. The recovered catalyst was used in the next cycle with new substrates. Each cycle followed the same procedure for catalyst recycling.

## RESULTS AND DISCUSSION

**Preparation.** Different possible reactions were carried out using $ZrCl_4$ and the $H_2BDC\text{-}C_5H_4NOS$ linker in DMF at different temperatures using four modulators (benzoic acid, acetic acid, trifluoroacetic acid, and formic acid).[58,59] A highly crystalline sample of **1** was achieved when a mixture of $ZrCl_4$, $H_2BDC\text{-}C_5H_4NOS$ linker, formic acid, and DMF in the required molar ratio was subjected to a solvothermal reaction at 120 °C for 1 day.

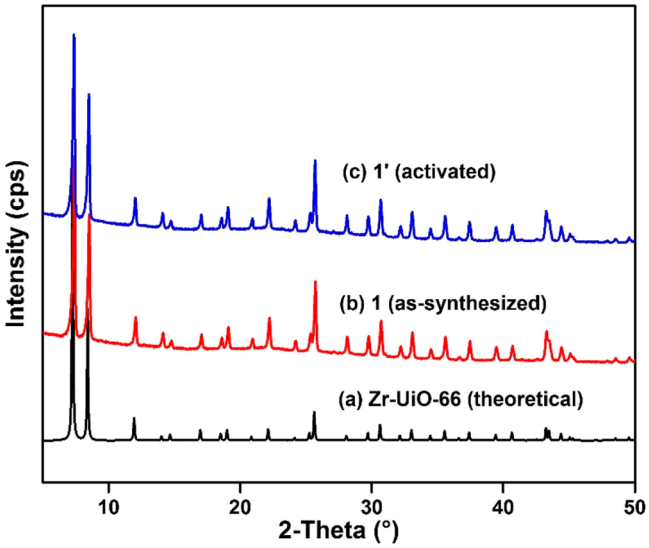


**Figure 1.** PXRD patterns of (a) Zr(IV)-based UiO-66 (theoretical), (b) **1** (experimental), and (c) **1′** (experimental).

**FT-IR Study.** The IR spectra of **1** and **1′** were recorded to confirm the presence of the linker molecule in the compounds. As described in Figure S4 in the Supporting Information, the very strong peak at 1586 $cm^{-1}$ is due to an asymmetric stretching vibration and the strong peak at 1423 $cm^{-1}$ is due to the presence of a symmetric stretching vibration of carboxylate linker molecules. Therefore, these results ensure the existence of the linker molecules within the frameworks of **1** and **1′**.[60,61] In the spectrum of the free linker molecule, the peak at 1654 $cm^{-1}$ is attributed to the carbonyl group from the amide moiety.[62] This peak was shifted to 1647 $cm^{-1}$ for both **1** and **1′**, indicating the incorporation of the amide linkage within the framework of the MOF.

**PXRD Analysis.** Figure 1 shows the PXRD patterns of **1** and **1′**. From the PXRD patterns, it is obvious that both compounds have the same peak intensity as well as the same peak positions as the theoretical peak pattern of the analogous UiO-66 compound.[63,64] Therefore, it is concluded that **1** has a UiO-66 framework topology. From Figure 1, it is also concluded that **1** is robust enough toward the activation conditions and the activated compound also has the UiO-66 framework.[63−65]


DOI: 10.1021/acs.inorgchem.9b02608
Inorg. Chem. XXXX, XXX, XXX−XXX

**Scheme 1. Reaction Scheme for the Ring Opening of Substrate 1 by Substrate 2 Using 1′ as a Heterogeneous Catalyst**

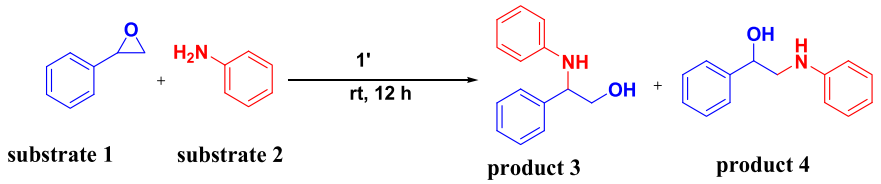


**Table 1. Optimization of Reaction Parameters for the Ring Opening of Substrate 1 by Substrate 2 Employing 1′ as a Heterogeneous Catalyst**[a]

| | | | selectivity (%)[c] | |
|---|---|---|---|---|
| entry | solvent | yield[b] (%) | 3 | 4 |
| 1 | ACN | 44 | 96 | 4 |
| 2 | THF | 23 | 87 | 13 |
| 3 | DCM | 54 | 93 | 7 |
| 4 | benzene | 51 | 94 | 6 |
| 5 | toluene | 67 | 95 | 5 |
| 6 | | 95 | 96 | 4 |
| 7 | | 2[d] | 100 | |

[a]Reaction conditions unless specified otherwise: substrate **1** (0.6 mmol), substrate **2** (0.5 mmol), solvent (1 mL), catalyst **1′** (15 mg), room temperature, 12 h. [b]Determined by GC using an internal standard method. [c]Determined by GC and GC-MS. [d]In the absence of catalyst **1′**.

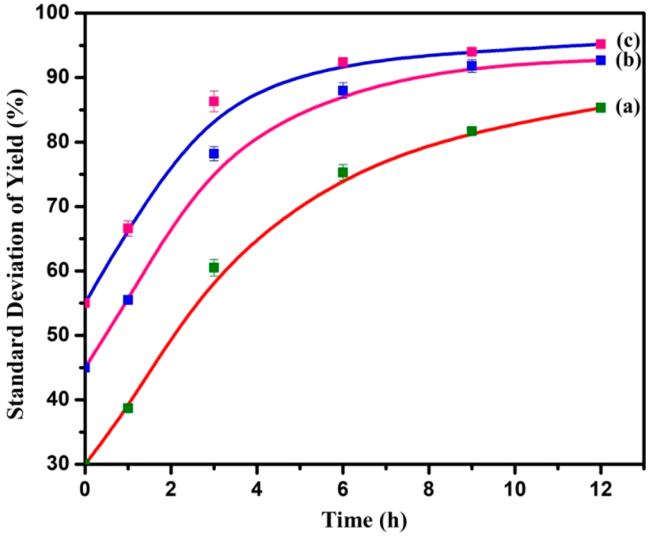


**Figure 2.** Effect of catalyst loading for the aminolysis of **1** by **2** in the presence of (a) 5 mg, (b) 10 mg, and (c) 15 mg of **1′**. Standard deviation analysis was performed by measuring four individual experiments for each catalyst loading.

**Structure Description.** The UiO-66 MOF with a Zr(IV) ion was discovered by Lillerud's group in 2008.[64] As demonstrated by Lillerud's group, the Zr-UiO-66 framework is composed of $[Zr_6O_4(OH)_4]^{12+}$ clusters in which every Zr(IV) ion is octacoordinated (square-antiprismatic geometry). 1,4-Benzenedicarboxylate (BDC) linker molecules interconnect one SBU with another one in the framework. A 3D cubic framework is obtained by interconnecting $Zr_6$ clusters with BDC linkers (12 linkers per cluster). The 3D framework possesses larger octahedral and smaller tetrahedral cages. Narrow triangular windows connect the two types of cages. For the present MOF (Figure S5 in the Supporting Information),

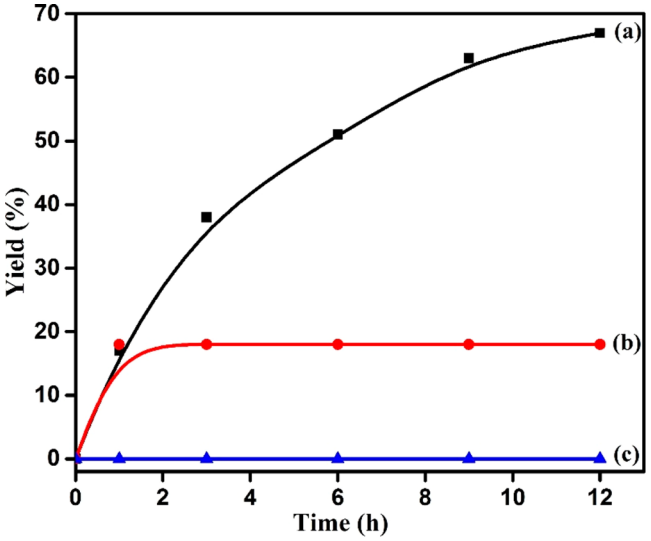


**Figure 3.** Time−yield plot for ring opening of substrate **1** by substrate **2** using **1′** as a heterogeneous solid catalyst: (a) with catalyst; (b) with filtering of the catalyst after 1 h; (c) without catalyst. Reaction conditions: substrate **1** (0.6 mmol), substrate **2** (0.5 mmol), toluene (1 mL), **1′** (15 mg), room temperature, 12 h.

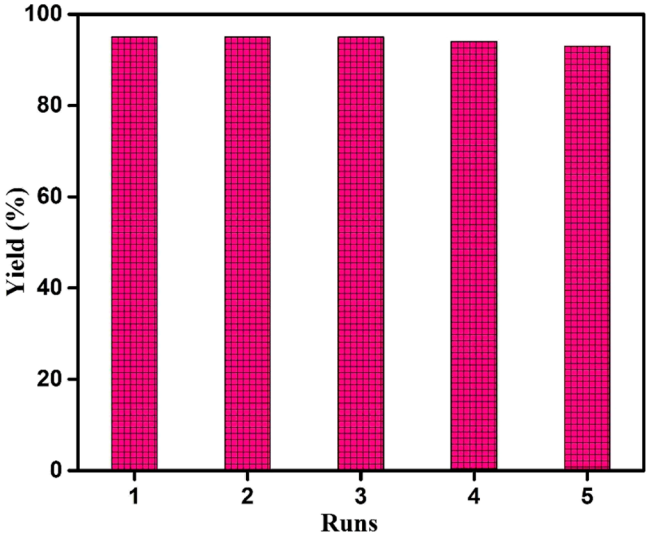


**Figure 4.** Reusability plot for ring opening of substrate **1** by substrate **2** using **1′** as a solid catalyst.

thiophene-2-carboxamide-functionalized BDC plays a role similar to that played by unfunctionalized BDC in the formation of the UiO-66 framework.[64,65] Figure S6 in the Supporting Information shows the pore size distribution plot for **1′**. This plot confirms that the microspores of **1′** are centered at 15.2 Å.

For structural analysis, the PXRD pattern of **1** was indexed. The derived lattice parameters are compared with those of the



DOI: 10.1021/acs.inorgchem.9b02608
Inorg. Chem. XXXX, XXX, XXX−XXX

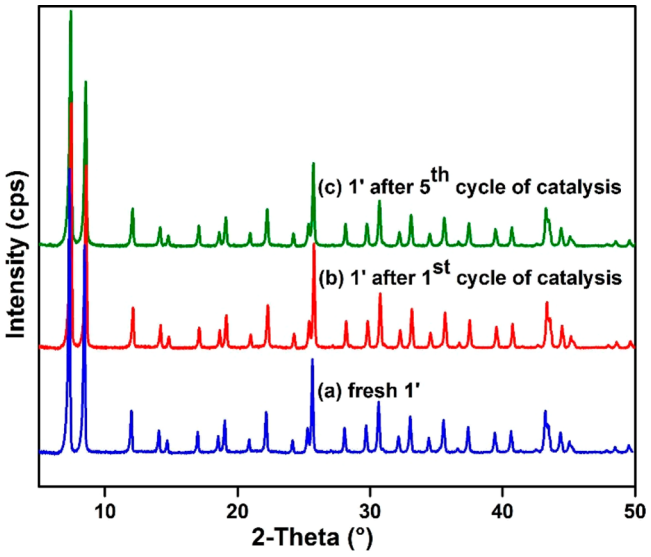


**Figure 5.** Comparison of the PXRD pattern of a fresh sample of **1′** (a) with that of the same sample recovered after the first (b) and fifth (c) cycles of catalysis.

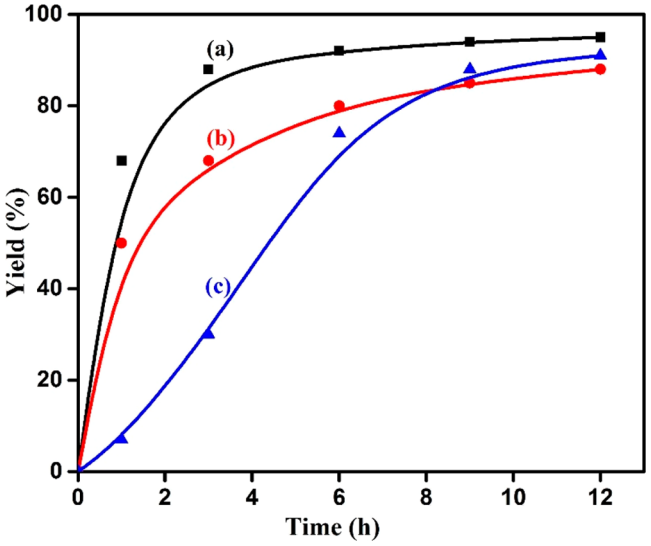


**Figure 6.** Time−yield plot for the ring opening of substrate **1** by substrate **2** using **1′** (a) and its corresponding homogeneous counterparts metal salt ($ZrCl_4$) (b) and linker ($H_2$BDC-(thiophene-2-carboxamido)) (c).

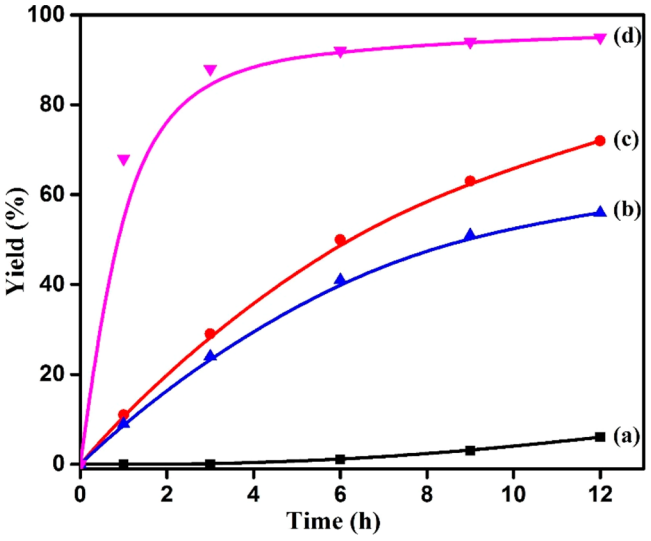


**Figure 7.** Time−yield plot for ring opening of substrate **1** by substrate **2** using different MOFs as solid heterogeneous catalysts: (a) $Cu_3(BTC)_2$; (b) Zr-UiO-66; (c) Fe(BTC); (d) **1′**.

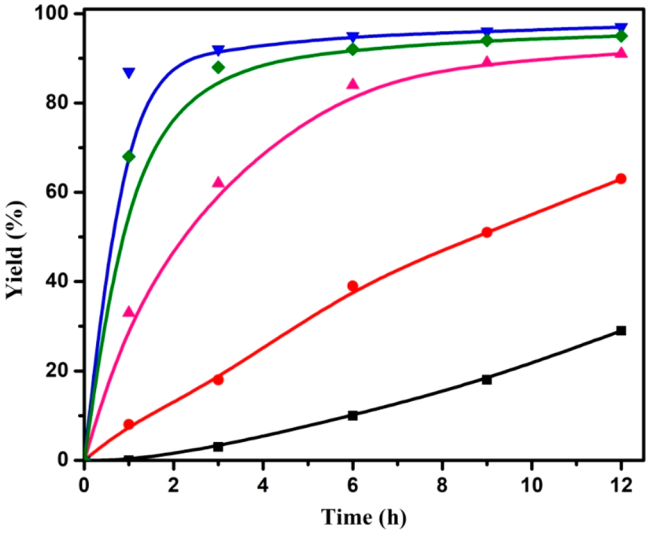


**Figure 8.** Time−yield plots for the aminolysis of substrate **1** by substrate **2** using different solid heterogeneous catalysts: (■) MIL-53(Al); (●) neutral $Al_2O_3$; (▲) $SiO_2$; (♦) **1′**; (▼) K10 montmorillonite clay.

reported unfunctionalized Zr-UiO-66 MOF in Table S1 in the Supporting Information.[59,63] The similarities in lattice parameters indicate that the structure of **1** is cubic and possesses a UiO-66 framework topology.[59,63] The structural similarity of **1** with Zr-UiO-66 was further confirmed by Pawley refinement (Figure S7 in the Supporting Information) with the PXRD pattern of **1**.

As indicated by indexing and Pawley refinement, the structure of **1** exhibits a cubic symmetry like the parent framework of UiO-66. This also means that the attached functional groups are fully distributed over different possible positions. Due to this inherent configurational and conformational disorder, the localization of the attached moieties by the Rietveld method is impossible. However, the structure of such variants of UiO-66 can be well modeled in a lower symmetry, as described for example, for UiO-66-$CO_2$H.[66] In such cases, the resulting model represents the pseudorhombohedral setting of the cubic unit cell with identical cell edges and all angles fixed to 60°. However, due to the attached functional groups, the actual symmetry of such a model is only triclinic *P*1. Thus, we modeled the structure of **1** starting with the reported model for UiO-66-$CO_2$H in triclinic symmetry, using the Materials Studio software suite.[67] Starting with the literature values for the unit cell parameters ($a = b = c =$ 14.7106 Å, $\alpha = \beta = \gamma = 60°$) of UiO-66-$CO_2$H, we deduced the values for **1** by Pawley refinement to be $a = b = c =$ 14.7174 Å with angles fixed to 60°. After these cell parameters were imposed, the functional $-CO_2H$ groups were replaced by thiophene-2-carboxamide moieties. Eventually, protons were added to the linker molecules and the model was fully relaxed by force-field calculations using the universal fore field UFF.[68] The calculated PXRD pattern for this resulting final model is in close agreement with the experimental data, as shown in Figure


DOI: 10.1021/acs.inorgchem.9b02608
Inorg. Chem. XXXX, XXX, XXX−XXX

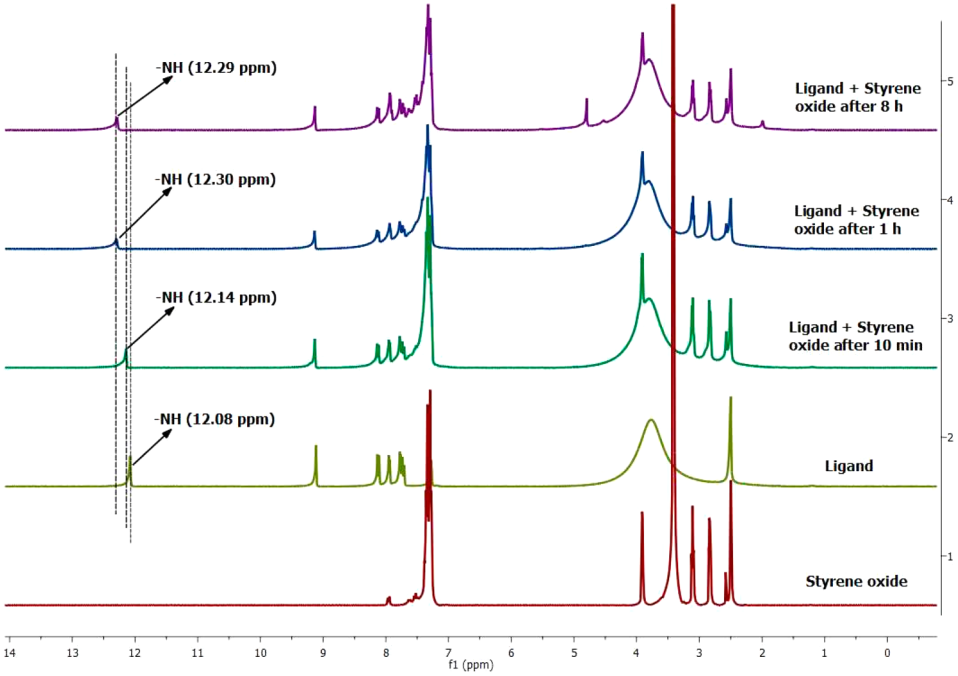


**Figure 9.** Stacked $^1$H NMR spectra of substrate **1**, the linker, and a physical mixture of linker and substrate **1** at different time intervals in DMSO-$d_6$.

S8 in the Supporting Information. The crystallographic information file is linked at the end of this paper.

**Thermal Stability.** The thermal stability of **1** and **1'** was determined by performing thermogravimetric (TG) experiments under argon atmosphere. From Figure S9 in the Supporting Information, it is inferred that both **1** and **1′** are stable up to 340 °C. The existing UiO-66 type MOFs have shown thermal stability similar to that of **1**.[69,70]

From Figure S9, it is noted that there are distinct weight loss stages for **1**. In the temperature range of 25−150 °C, there was the first weight loss of 2.9 wt % (calcd 2.9 wt %) due to the loss of 4.5 water molecules. The second weight loss was found to be 9.2 wt % (calcd 9.3 wt %) due to the loss of 3.5 DMF molecules. The linker molecules start to be eliminated from the framework of **1** beyond 340 °C. Therefore, it is confirmed that **1** is stable up to 340 °C. The desolvated sample (**1′**) adsorbs moisture when it is stored in an air atmosphere. As a result, it shows a weight loss of 2.7 wt % in the region of 25−150 °C for the removal of adsorbed water molecules.

**Chemical Stability.** Chemical stability is one of the important factors which is crucial for the practical application of a MOF. The chemical stability of **1′** was ascertained by treating with water, 1 M HCl, glacial acetic acid, and 0.01 M NaOH solutions for 14 h. Subsequently, the solid residues were obtained by filtration and they were placed in an oven maintained at 100 °C for 6 h. PXRD patterns were collected with the dry solids. Although the structural integrity of **1′** was lost upon treatment with 0.01 M NaOH solution, it remained stable in water, 1 M HCl, and glacial acetic acid, as evidenced by PXRD patterns (Figure S10 in the Supporting Information). These results point out that the chemical stability of **1′** is quite satisfactory and is comparable with that of the previously reported UiO-66 MOFs.[59,70]

**$N_2$ Sorption Study.** The activated compound **1′** was used to carry out $N_2$ physisorption analysis. The obtained type I type $N_2$ sorption isotherms are shown in Figure S11 in the Supporting Information. From this physisorption analysis, the surface area and micropore volume of the material were derived as 781 $m^2/g$ and 0.44 $cm^3/g$ at a $p/p_0$ value of 0.5, respectively. The shape of the $N_2$ sorption curves and the value of the pore volume revealed that **1′** is a microporous material. Compound **1′** is comparable with the reported parent and functionalized UiO-66 MOF with regard to surface area and micropore volume.[59,70,71]

**Catalytic Activity.** The catalytic performance of **1′** was investigated in the aminolysis of epoxides. Styrene oxide (substrate **1**) and aniline (substrate **2**) were chosen as representative substrates. This reaction afforded two regioisomers, and they are shown in Scheme 1 as products **3** and **4**. The achieved results are provided in Table 1. The analysis of the observed products was executed by GC-MS and $^1$H NMR methods (Figures S12−S49 in the Supporting Information). The ring-opening reaction between **1** and **2** using **1′** as a catalyst in various solvents such as ACN (acetonitrile), THF (tetrahydrofuran), DCM (dichloromethane), benzene, and toluene exhibited moderate yields between 23 and 67% after stirring for 12 h at ambient temperature (Table 1, entries 1−5). In contrast, the reaction of **1** and **2** with **1′** as a solid catalyst afforded 95% yield under solvent-free conditions at ambient temperature after 12 h (Table 1, entry 6). In contrast, only 2% conversion was obtained under identical conditions when a control experiment was conducted in the absence of catalyst (Table 1, entry 7). In all of these cases, the use of **1′** as a solid catalyst showed the formation of **3** as the major product. These experiments clearly suggest that the reaction is promoted solely by **1′** as a catalyst in affording **3** as the major product. Then, the next logical move was to investigate the influence of catalyst loading of this reaction under identical conditions. Figure 2 provides the time−yield profile for the ring-opening reaction of substrate **1** by substrate **2** to obtain the desired product **3** by observing enhancement in the initial reaction rate as a function of catalyst


DOI: 10.1021/acs.inorgchem.9b02608
Inorg. Chem. XXXX, XXX, XXX−XXX

**Table 2. Ring Opening of Substrate 1 by Various Aryl and Alkyl Amine Substrates Using 1′ as a Solid Heterogeneous Catalyst[a]**

| Entry | Amine | Regioisomer | | Yield[b] (%) | Selectivity[c] | |
|---|---|---|---|---|---|---|
| | | Isomer I | Isomer II | | I | II |
| 1 |  | 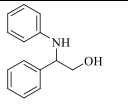 | 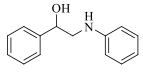 | 95 | 96 | 4 |
| 2 |  | 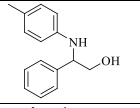 | 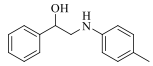 | 95 | 95 | 5 |
| 3 |  | 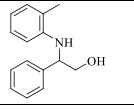 | 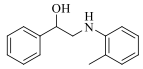 | 95 | 96 | 4 |
| 4 | 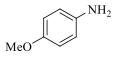 | 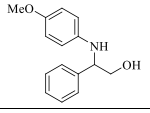 | 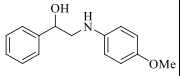 | 94 | 95 | 5 |
| 5 |  | 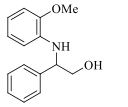 | 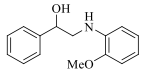 | 95 | 96 | 4 |
| 6 |  | 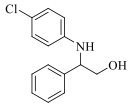 | 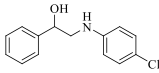 | 95 | 97 | 3 |
| 7 |  | 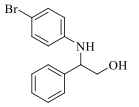 | 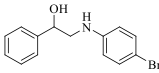 | 94 | 98 | 2 |
| 8 |  | 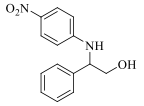 | 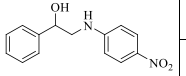 | 31 | 97 | 3 |
| | | | | 89[d] | 96 | 4 |
| 9 | 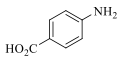 | 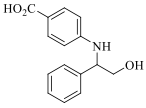 | 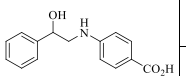 | 44 | 100 | - |
| | | | | 53[d] | 100 | - |
| 10 |  | 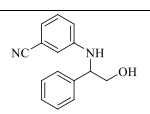 | 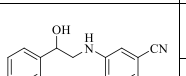 | 82 | 97 | 3 |
| | | | | 93[e] | 98 | 2 |
| 11 |  | 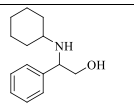 | 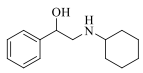 | 66 | 17 | 83 |
| | | | | 92[e] | 29 | 71 |
| 12 |  | 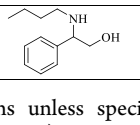 | 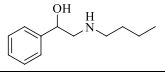 | 74 | 47 | 53 |
| | | | | 89[e] | 51 | 49 |

[a]Reaction conditions unless specified otherwise: substrate **1** (0.6 mmol), amine (0.5 mmol), catalysts **1′** (15 mg), room temperatue, 12 h. [b]Determined by GC using an internal standard method. [c]Determined by GC and GC-MS. [d]At 60 °C for 24 h. [e]At 60 °C for 12 h.

loading. This observation is due to the availability of a high population of active sites with higher catalyst loading.

Figure 3 presents a time−yield profile for the conversion of **1** to **3** and **4** by **2** using **1′** as a solid catalyst and a control experiment without **1′** in toluene at room temperature. These catalytic results suggest that the presence of a catalyst is required for this reaction even in the presence of solvents. Further, to validate whether the present catalytic method is

**Table 3. Ring Opening of Other Epoxide Substrates by Substrate 2 Using 1′ as a Heterogeneous Solid Catalyst[a]**

| Entry | Epoxide | Regioisomer | | Yield[b] (%) | Selectivity[c] | |
|---|---|---|---|---|---|---|
| | | Isomer I | Isomer II | | I | II |
| 1 |  | 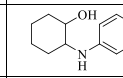 | - | 97 | - | - |
| 2 |  | 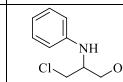 |  | 93 | - | 100 |
| 3 |  |  |  | 79 | 46 | 54 |
| | | | | 88[d] | 48 | 52 |

[a]Reaction conditions unless specified otherwise: epoxide (0.6 mmol), substrate **2** (0.5 mmol), catalyst **1′** (15 mg), room temperature, 12 h. [b]Determined by GC using an internal standard method. [c]Determined by GC and GC-MS. [d]At 60 °C.

inherently heterogeneous in nature, the catalyst was taken out from reaction mixture after 1 h when the conversion of **1** was about 18%. Then, the reaction in the absence of **1′** was continued under identical experimental conditions for the remaining time (Figure 3). The observed results suggest that the rate of reaction became completely constant after elimination of the catalyst from the reaction vessel. Further, the filtrate of the reaction mixture was investigated by ICP-AES, which verified the absence of zirconium (below the detection limit). These results convincingly demonstrate that the reaction is heterogeneous in nature. Moreover, the catalyst was conveniently retrieved from the reaction mixture by filtration and used for five cycles without any decay in its catalytic performance (Figure 4). The five-time used catalyst showed a crystalline pattern (Figure 5) identical with that of the fresh solid through PXRD analysis (Figure 5), thus verifying the structural integrity of **1′** under the reaction conditions. Moreover, the crystalline nature of **1′** was verified by FE-SEM analysis (Figures S50 and S51 in the Supporting Information) and an unaltered morphology of **1′** after catalysis was observed in comparison to its fresh sample. In addition, EDX elemental analysis and EDX mapping revealed no changes in the elemental composition of **1′** before and after catalysis, as shown in Figures S52−S55 in the Supporting Information.

The nature of active sites was also examined in **1′** by comparing its activity with those of corresponding metal salt and linker. The results achieved are displayed in Figure 6. The activity of **1′** is significantly higher in comparison to $ZrCl_4$ (metal component) and 2-(thiophene-2-carboxamido)-benzene-1,4-dicarboxylic acid (linker). This may be attributed to the presence of dual active sites in **1′** through the metal node (Lewis acidic site) and the 2-(thiophene-2-carboxamido) functionalized linker (pseudo Lewis acidic site) for the ring opening of **1**. This hypothesis was verified by conducting a masking experiment with pyridine. The activities of $ZrCl_4$, linker, and **1′** were completely quenched by the introduction of pyridine to the reaction mixture. These results unambiguously prove that pyridine behaves as a Lewis base by coordinating strongly to the metal ion like a $\sigma$ bond, thus inhibiting the interactions of substrate **1** with the metal centers.[72] Furthermore, the activities of **1′** and linker were quenched by pyridine due to the formation of hydrogen bonding between the −NH group of linker and N atom of pyridine.[73]



DOI: 10.1021/acs.inorgchem.9b02608
Inorg. Chem. XXXX, XXX, XXX−XXX

**Scheme 2. Possible Mechanism for the Ring Opening of Substrate 1 by Substrate 2 through (a) Metal Sites ($Zr^{4+}$) and (b) Thiophene-2-carboxamido Linker in 1′**

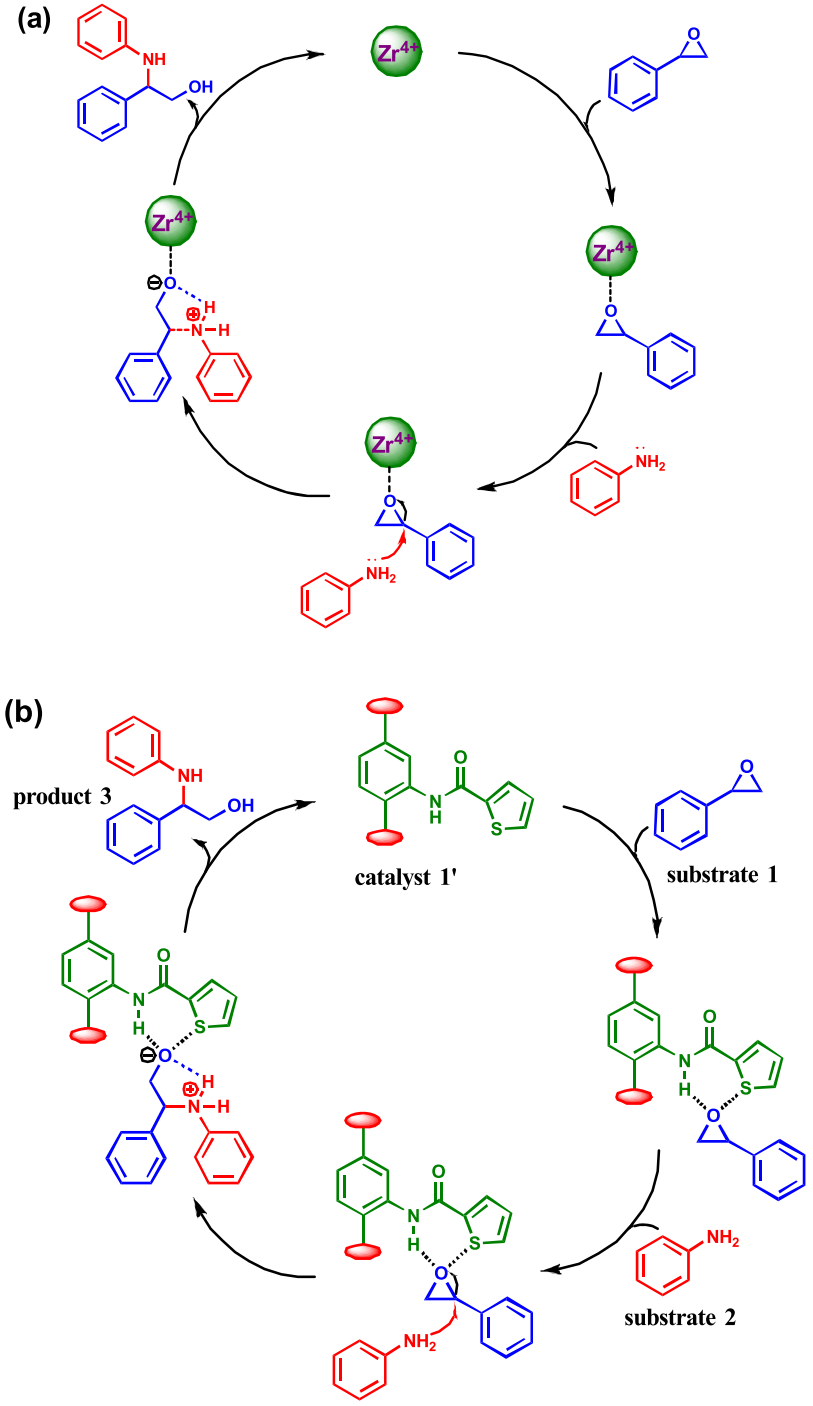


The activity of **1′** was also screened with a series of MOFs possessing Lewis acidic sites such as Fe(BTC), $Cu_3(BTC)_2$, and Zr-UiO-66, and the observed results are shown in Figure 7. These data prove that **1′** has better catalytic performance in comparison to other tested MOFs under identical conditions. This superior performance of **1′** could be due to the high population of active sites in comparison to the other catalysts. Interestingly, the enhanced catalytic performance of **1′** in comparison to Zr-UiO-66 is due to the operation of dual active sites in **1′**.

In addition to comparing the activity of **1′** with other related MOFs, the catalytic performance of **1′** was also compared with some of the conventional catalysts such as MIL-53(Al), neutral $Al_2O_3$, $SiO_2$, and K10 montmorillonite clay employed for the ring opening of epoxides by amines under similar conditions. The observed catalytic data are given in Figure 8. K10 montmorillonite clay provided slightly higher activity than **1′**, but this activity difference is due to the difference in the structure and active sites. Furthermore, the reactants reach the active sites without having any diffusion limitation in clay, while the use of **1′** impedes the diffusion of reactants. On other


DOI: 10.1021/acs.inorgchem.9b02608
Inorg. Chem. XXXX, XXX, XXX−XXX

hand, the activity of **1′** was comparable to that of $SiO_2$, while the activities of $Al_2O_3$ and MIL-53(Al) were significantly lower in comparison to **1′**. Hence, it is very difficult to compare the activity of **1′** with those of other conventional catalysts, since the activity of a solid depends on many factors such as structure of the catalyst, active sites, diffusion limitation, and others. The activity of **1′** may be higher or lower in comparison to conventional catalysts, but the objective of this work is not to rank the present catalyst in the series but rather to demonstrate the ability of **1′** to promote the ring opening of epoxides by amines.

In order to enlarge the scope of our catalyst, aminolysis of epoxides was performed with various amine substrates catalyzed by **1′** using the optimized reaction parameters. The obtained catalytic results are presented in Table 2. The reaction of **1** with **2** in the presence of **1′** afforded a 95% yield with the *β*-amino alcohol as the major regioisomer (Table 2, entry 1). Similarly, 4- and 2-methylanilines were reacted effectively with **1** to provide the respective products in 95% yields under identical conditions (Table 2, entries 2 and 3). Further, the aminolysis reaction of **1** by 4- and 2-methoxyanilines showed 94 and 95% yields, respectively, showing an isomer identical with that of aniline (Table 2, entries 4 and 5). In addition, the reaction of **1** with 4-chloro- and 4-bromoanilines exhibited the corresponding *β*-amino alcohols in 95 and 94% yields, respectively, under the optimized reaction conditions (Table 2, entries 6 and 7). On the other side, the aminolysis of **1** by 4-nitroaniline showed a 31% yield at room temperature after 12 h, whereas the yield increased to 89% at 60 °C after 24 h (Table 2, entry 8). This decreased rate with 4-nitroaniline may be due to the poor nucleophilic character of the amino group caused by the existence of an electron-withdrawing nitro group. A similar behavior was also witnessed for the aminolysis reaction between **1** and 4-aminobenzoic acid (Table 2, entry 9). In addition, the reaction between 3-cyanoaniline and **1** with **1′** as a solid catalyst exhibited an 82% yield at ambient temperature and a 93% yield at 60 °C after 12 h (Table 2, entry 10).

Furthermore, the reaction of **1** and aminocyclohexane using **1′** as a solid catalyst afforded the secondary alcohol (isomer **II**) as the major product at room temperature; however, the yield increased to 92% at 60 °C after 12 h (Table 2, entry 11). This inverse selectivity may be due to the steric hindrance of the cyclohexane ring which prefers to attack the methylene carbon in **1**. Interestingly, the aminolysis reaction of **1** and *n*-butylamine exhibited an equal ratio of regioisomers either at room temperature or at 60 °C (Table 2, entry 12).

Furthermore, ring opening of other epoxide substrates with **2** using **1′** as a catalyst was also tested under identical conditions. The obtained results are presented in Table 3. The reaction of cyclohexene oxide with **2** in the presence of **1′** afforded a single product in 97% yield at ambient temperature (Table 3, entry 1). Further, the aminolysis of epichlorohydrin with **2** using **1′** as a solid catalyst showed the secondary alcohol as the only product (Table 3, entry 2). This may be explained due to the steric nature of the chlorine atom. Finally, mixtures of regioisomers with equal selectivity were obtained for the reaction between isobutylene oxide and substrate **2** with **1′** as a catalyst at room temperature or at 60 °C (Table 3, entry 3).

A suitable reaction mechanism is proposed for the aminolysis of substrate **1** by substrate **2** with **1′** as a solid catalyst (Scheme 2). As discussed earlier, there are two types of active sites in **1′**: namely, the metal sites ($Zr^{4+}$) and the linker. Hence, the mechanism is proposed by involving both active sites. Scheme 2a shows the interaction of substrate **1** with **1′** through oxygen by decreasing the electron density in the carbon attached to phenyl, thus favoring nucleophilic attack. This carbon site was attacked by **2** to give the expected product **3**. This mechanism is in agreement with earlier literature reports involving metal sites as active sites.[74−77]

On the other hand, Scheme 2b provides the possible mechanism through the linker installed in **1′**. The interaction of substrate **1** with catalyst **1′** occurs through the weak coordination of an oxygen atom of substrate **1** with the N−H and thiophene moieties in **1′**. This interaction decreases the electron density at the secondary carbon in substrate **1**, thus favoring the nucleophilic attack by substrate **2** to provide an intermediate as shown in Scheme 2b. This further rearranges to provide the expected product in a major proportion. Furthermore, the formation of another product is also possible through the attack of a nucleophile (substrate **2**) at the methylene carbon under identical reaction conditions.

One of the proposed intermediates in Scheme 2b is the interaction of substrate **1** through the oxygen with **1′** of an N−H bond. In order to prove this interaction, $^1$H NMR spectra were recorded for the linker, substrate **1**, and a physical mixture of the linker with substrate **1**. The observed results are shown in Figure 9. The N−H proton in the linker is seen at 12.08 ppm, while upon addition of substrate **1**, this peak was shifted to downfield to 12.14 ppm after 10 min and further to 12.30 and 12.29 ppm after 1 and 8 h, respectively. These results are in close agreement with an earlier report.[78] Furthermore, an additional control experiment was performed to prove the proposed mechanism with deuterated methanol ($CD_3OD$) as a nucleophile for the ring opening of substrate **1** under similar experimental conditions. The analysis of the reaction mixture by GC-MS clearly indicates the formation of a product with an $m/z$ value of 156 (Figure S56 in the Supporting Information), whereas the $m/z$ value is 152 for $CH_3OH$ (Figure S57 in the Supporting Information). These experiments confirm that the hydrogen transfer occurring from the protonated intermediate to the final product originates from the nucleophile, as shown in Scheme 2.

## CONCLUSIONS

We have demonstrated the synthesis and characterization of the new 2-(thiophene-2-carboxamido)benzene-1,4-dicarboxylic acid linker and successfully utilized it for the synthesis of a Zr(IV)-based UiO-66 MOF. The MOF was synthesized using a traditional solvothermal method and characterized using PXRD, FT-IR, TG, and BET analysis. The specific BET surface area of **1′** derived from nitrogen physisorption experiment was 781 $m^2/g$. The material showed high chemical stability (in acetic acid, 1 M HCl, and water) as well as thermal stability (up to 340 °C). Material **1′** was employed as a heterogeneous solid catalyst for the ring opening of epoxides by amines. Catalyst **1′** showed higher yields of the ring-opened products and broad substrate scope for both epoxides and amines. The catalyst displayed better activity than existing Lewis acidic MOF catalysts such as $Cu_3(BTC)_2$, Fe(BTC), and Zr-UiO-66. The exclusive role of **1′** in the catalytic reaction was verified by executing control experiments with the free linker and the zirconium salt and without catalyst **1′**. The reusability of the catalyst was illustrated up to five cycles. A plausible mechanism for the catalytic reaction has been also provided.



DOI: 10.1021/acs.inorgchem.9b02608
Inorg. Chem. XXXX, XXX, XXX−XXX

## ■ ASSOCIATED CONTENT

### Supporting Information

The Supporting Information is available free of charge at https://pubs.acs.org/doi/10.1021/acs.inorgchem.9b02608.

Mass, NMR, EDX, and FT-IR spectra, simulated structure, TG curves, pore size distribution plot, PXRD patterns, nitrogen sorption isotherms, indexing results, and FE-SEM images (PDF)

## ■ AUTHOR INFORMATION


### Corresponding Authors

*A.D.: e-mail, admguru@gmail.com.

*S.B.: e-mail, sbiswas@iitg.ernet.in; tel, (+)91-3612583309; fax, (+)91-3612582349.

### ORCID

Helge Reinsch: 0000-0001-5288-1135

Amarajothi Dhakshinamoorthy: 0000-0003-0991-6608

Shyam Biswas: 0000-0001-7103-9939


### Author Contributions

The manuscript was written through contributions of all authors. All authors have given approval to the final version of the manuscript.

### Notes

The authors declare no competing financial interest.

## ■ ACKNOWLEDGMENTS

S.B. and A.D. are grateful for financial assistance from Science and Engineering Research Board (SERB) through grant nos. EEQ/2016/000012 and EMR/2016/006500, respectively. A.D. is grateful to the University Grants Commission for an Assistant Professorship award.

## ■ REFERENCES


(1) Posner, G. H.; Rogers, D. Z. Organic Reactions at Alumina Surfaces.' Mild and Selective Opening of Epoxides by Alcohols, Thiols, Benzeneselenol, Amines, and Acetic Acid. *J. Am. Chem. Soc.* **1977**, *99*, 8208−8214.

(2) Liebscher, J.; Jin, S.; Otto, A.; Woydowski, K. Synthetic application of chiral pool derived heterocycles. *J. Heterocycl. Chem.* **2000**, *37*, 509−518.

(3) Vilotijevic, I.; Jamison, T. F. Epoxide-Opening Cascades in the Synthesis of Polycyclic Polyether Natural Products. *Angew. Chem., Int. Ed.* **2009**, *48*, 5250−5281.

(4) Bonollo, S.; Lanari, D.; Vaccaro, L. Ring-Opening of Epoxides in Water. *Eur. J. Org. Chem.* **2011**, *2011*, 2587−2598.

(5) Kopka, K.; Wagner, S.; Riemann, B.; Law, M. P.; Puke, C.; Luthra, S. K.; Pike, V. W.; Wichter, T.; Schmitz, W.; Schober, O.; Schäfers, M. Design of new $\beta_1$-selective adrenoceptor ligands as potential radioligands for in vivo imaging. *Bioorg. Med. Chem.* **2003**, *11*, 3513−3527.

(6) Ager, D. J.; Prakash, I.; Schaad, D. R. 1,2-Amino Alcohols and Their Heterocyclic Derivatives as Chiral Auxiliaries in Asymmetric Synthesis. *Chem. Rev.* **1996**, *96*, 835−876.

(7) Azizi, N.; Mirmashhori, B.; Saidi, M. R. Lithium perchlorate promoted highly regioselective ring opening of epoxides under solvent-free conditions. *Catal. Commun.* **2007**, *8*, 2198−2203.

(8) Zhang, J.-D.; Yang, X.-X.; Jia, Q.; Zhao, J.-W.; Gao, L.-L.; Gao, W.-C.; Chang, H.-H.; Wei, W.-L.; Xu, J.-H. Asymmetric ring opening of racemic epoxides for enantioselective synthesis of (S)-$\beta$-amino alcohols by a cofactor self-sufficient cascade biocatalysis system. *Catal. Sci. Technol.* **2019**, *9*, 70−74.

(9) Malkov, A. V.; Kabeshov, M. A.; Bella, M.; Kysilka, O.; Malyshev, D. A.; Pluháčková, K.; Kočovský, P. Vicinal Amino Alcohols as Organocatalysts in Asymmetric Cross-Aldol Reaction of Ketones: Application in the Synthesis of Convolutamydine A. *Org. Lett.* **2007**, *9*, 5473−5476.

(10) Andrés, J. M.; Barrio, R.; Martínez, M. A.; Pedrosa, R.; Pérez-Encabo, A. Synthesis of Enantiopure syn-$\beta$-Amino Alcohols. A Simple Case of Chelation-Controlled Additions of Diethylzinc to $\alpha$-(Dibenzylamino) Aldehydes. *J. Org. Chem.* **1996**, *61*, 4210−4213.

(11) Jung, M. E.; Yi, S. W. Synthesis of threo-b-aminoalcohols from aminoaldehydes via chelation-controlled additions. Total synthesis of L-threo sphingosine and safingol. *Tetrahedron Lett.* **2012**, *53*, 4216−4220.

(12) Bergmeier, S. C. The Synthesis of Vicinal Amino Alcohols. *Tetrahedron* **2000**, *56*, 2561−2576.

(13) Tanaka, K.; Kinoshita, M.; Kayahara, J.; Uebayashi, Y.; Nakaji, K.; Morawiak, M.; Urbanczyk-Lipkowska, Z. Asymmetric ring-opening reaction ofmesoepoxides with aromatic amines using homochiral metal−organic frameworks as recyclable heterogeneous catalysts. *RSC Adv.* **2018**, *8*, 28139−28146.

(14) Chen, W.; Zhou, Z.-H.; Chen, H.-B. Efficient synthesis of chiral benzofuryl $\beta$-amino alcohols via a catalytic asymmetric Henry reaction. *Org. Biomol. Chem.* **2017**, *15*, 1530−1536.

(15) Kinage, A. K.; Upare, P. P.; Shivarkar, A. B.; Gupte, S. P. Highly Regio-Selective Synthesis of $\beta$-Amino Alcohol by Reaction with Aniline and Propylene Carbonate in Self Solvent System over Large Pore Zeolite Catalyst. *Green Sustainable Chem.* **2011**, *01*, 76−84.

(16) Métro, T.-X.; Appenzeller, J.; Pardo, D. G.; Cossy, J. Highly Enantioselective Synthesis of $\beta$-Amino Alcohols. *Org. Lett.* **2006**, *8*, 3509−3512.

(17) Kamble, V. T.; Joshi, N. S. Synthesis of $\beta$-amino alcohols by ring opening of epoxides with amines catalyzed by cyanuric chloride under mild and solvent-free conditions. *Green Chem. Lett. Rev.* **2010**, *3*, 275−281.

(18) Bhagavathula, D. S.; Boddeti, G.; Venu, R. A Brief Review on Synthesis of $\beta$-amino Alcohols by Ring Opening of Epoxides. *Res. Rev.: J. Chem.* **2017**, *6*, 27−46.

(19) Michael, J. P. Indolizidine and quinolizidine alkaloids. *Nat. Prod. Rep.* **2001**, *18*, 520−542.

(20) De Cree, J.; Geukens, H.; Leempoels, J.; Verhaegen, H. Haemodynamic effects in man during exercise of a single oral dose of narbivolol (R 67555), a new beta-1-adrenoceptor blocking agent: A comparative study with atenolol, pindolol, and propranolol. *Drug Dev. Res.* **1986**, *8*, 109−117.

(21) Kamboj, R.; Bhadani, A.; Singh, S. Synthesis of$\beta$-Amino Alcohols from Terminal Epoxy Fatty Acid Methyl Ester. *Ind. Eng. Chem. Res.* **2011**, *50*, 8379−8383.

(22) Julião, D.; Barbosa, A. D. S.; Peixoto, A. F.; Freire, C.; Castro, B. D.; Balula, S. S.; Cunha-Silva, L. Improved catalytic performance of porous metal−organic frameworks for the ring opening of styrene oxide. *CrystEngComm* **2017**, *19*, 4219−4226.

(23) Varshney, H.; Ahmad, A.; Rauf, A. Ring Opening of Epoxy Fatty Esters by Nucleophile to Form the Derivatives of Substituted $\beta$-Amino Alcohol. *Food Nutr. Sci.* **2013**, *04*, 21−24.

(24) Bansal, S.; Kumar, Y.; Pippal, P.; Das, D. K.; Pramanik, P.; Singh, P. P. An efficient method for regioselective ring opening of epoxides by amines under microwave irradiation using $Bi(NO_3)_3 \cdot 5H_2O$ as a catalyst. *New J. Chem.* **2017**, *41*, 2668−2671.

(25) Azizi, N.; Saidi, M. R. Highly Chemoselective Addition of Amines to Epoxides in Water. *Org. Lett.* **2005**, *7*, 3649−3651.

(26) Lee, M.; Lamb, J. R.; Sanford, M. J.; LaPointe, A. M.; Coates, G. W. Nucleophilic ring opening of trans-2,3-disubstituted epoxides to $\beta$-amino alcohols with catalyst-controlled regioselectivity. *Chem. Commun.* **2018**, *54*, 12998−13001.

(27) Wu, J.; Xia, H.-G. Tertiary amines as highly efficient catalysts in the ring-opening reactions of epoxides with amines or thiols in $H_2O$: expeditious approach to b-amino alcohols and b-aminothioethers. *Green Chem.* **2005**, *7*, 708−710.

(28) Baskaran, T.; Joshi, A.; Kamalakar, G.; Sakthivel, A. A solvent free method for preparation of $\beta$-amino alcohols by ring opening of epoxides with amines using MCM-22 as a catalyst. *Appl. Catal., A* **2016**, *524*, 50−55.




DOI: 10.1021/acs.inorgchem.9b02608
*Inorg. Chem.* XXXX, XXX, XXX−XXX

(29) Nobuta, T.; Xiao, G.; Ghislieri, D.; Gilmore, K.; Seeberger, P. H. Continuous and convergent access to vicinyl amino alcohols. *Chem. Commun.* **2015**, *51*, 15133−15136.
(30) Tobisch, S. Computational Mechanistic Elucidation of the Intramolecular Aminoalkene Hydroamination Catalysed by Iminoanilide Alkaline-Earth Compounds. *Chem. - Eur. J.* **2015**, *21*, 6765−6779.
(31) Aramesh, N.; Yadollahi, B.; Mirkhani, V. Fe(III) substituted Wells−Dawson type polyoxometalate: An efficient catalyst for ring opening of epoxides with aromatic amines. *Inorg. Chem. Commun.* **2013**, *28*, 37−40.
(32) Chini, M.; Crotti, P.; Macchia, F. Metal salts as new catalysts for mild and efficient aminolysis of oxiranes. *Tetrahedron Lett.* **1990**, *31*, 4661−4664.
(33) Papini, A.; Ricci, A.; Taddei, M.; Seconi, G.; Dembech, P. Regiospecific conversion of oxiranes, oxetanes, and lactones into difunctional nitrogen compounds via aminosilanes and aminostannanes. *J. Chem. Soc., Perkin Trans. 1* **1984**, *0*, 2261−2265.
(34) Rani, P.; Srivastava, R. Nucleophilic addition of amines, alcohols, and thiophenol with epoxide/olefin using highly efficient zirconium metal organic framework heterogeneous catalyst. *RSC Adv.* **2015**, *5*, 28270−28280.
(35) Deyrup, J. A.; Moyer, C. L. 1,2,3-oxathiazolidines. Heterocyclic system. *J. Org. Chem.* **1969**, *34*, 175−179.
(36) Otera, J.; Niibo, Y.; Tatsumi, N.; Nozaki, H. Organotin phosphate condensates as a catalyst of selective ring-opening of oxiranes by alcohols. *J. Org. Chem.* **1988**, *53*, 275−278.
(37) Zhou, H.-C.; Long, J. R.; Yaghi, O. M. Introduction to Metal−Organic Frameworks. *Chem. Rev.* **2012**, *112*, 673−674.
(38) Bradshaw, D.; Garai, A.; Huo, J. Metal−organic framework growth at functional interfaces: thin films and composites for diverse applications. *Chem. Soc. Rev.* **2012**, *41*, 2344−2381.
(39) Karmakar, A.; Desai, A. V.; Ghosh, S. K. Ionic metal-organic frameworks (iMOFs): Design principles and applications. *Coord. Chem. Rev.* **2016**, *307*, 313−341.
(40) Chughtai, A. H.; Ahmad, N.; Younus, H. A.; Laypkov, A.; Verpoort, F. Metal−organic frameworks: versatile heterogeneous catalysts for efficient catalytic organic transformations. *Chem. Soc. Rev.* **2015**, *44*, 6804−6849.
(41) Pal, T. K.; De, D.; Senthilkumar, S.; Neogi, S.; Bharadwaj, P. K. A Partially Fluorinated, Water-Stable Cu(II)−MOF Derived via Transmetalation: Significant Gas Adsorption with High CO2 Selectivity and Catalysis of Biginelli Reactions. *Inorg. Chem.* **2016**, *55*, 7835−7842.
(42) Gupta, A. K.; De, D.; Tomar, K.; Bharadwaj, P. K. A Cu(II) metal−organic framework with significant $H_2$ and $CO_2$ storage capacity and heterogeneous catalysis for the aerobic oxidative amination of $C(sp_3)$−H bonds and Biginelli reactions. *Dalton Trans.* **2018**, *47*, 1624−1634.
(43) Gole, B.; Sanyal, U.; Banerjee, R.; Mukherjee, P. S. High Loading of Pd Nanoparticles by Interior Functionalization of MOFs for Heterogeneous Catalysis. *Inorg. Chem.* **2016**, *55*, 2345−2354.
(44) Sharma, S.; Ghosh, S. K. Metal−Organic Framework-Based Selective Sensing of Biothiols via Chemidosimetric Approach in Water. *ACS Omega* **2018**, *3*, 254−258.
(45) Das, A.; Biswas, S. A multi-responsive carbazole-functionalized Zr(IV)-based metal-organic framework for selective sensing of Fe(III), cyanide and p-nitrophenol. *Sens. Actuators, B* **2017**, *250*, 121−131.
(46) Lustig, W. P.; Mukherjee, S.; Rudd, N. D.; Desai, A. V.; Li, J.; Ghosh, S. K. Metal−organic frameworks: functional luminescent and photonic materials for sensing applications. *Chem. Soc. Rev.* **2017**, *46*, 3242−3285.
(47) Karmakar, A.; Kumar, N.; Samanta, P.; Desai, A. V.; Ghosh, S. K. A Post-Synthetically Modified MOF for Selective and Sensitive Aqueous-Phase Detection of Highly Toxic Cyanide Ions. *Chem. - Eur. J.* **2016**, *22*, 864−868.
(48) Wang, L.; Zheng, M.; Xie, Z. Nanoscale metal−organic frameworks for drug delivery: a conventional platform with new promise. *J. Mater. Chem. B* **2018**, *6*, 707−717.
(49) Gao, Y.; Broersen, R.; Hageman, W.; Yan, N.; Mittelmeijer-Hazeleger, M. C.; Rothenberg, G.; Tanase, S. High proton conductivity in cyanide-bridged metal−organic frameworks: understanding the role of water. *J. Mater. Chem. A* **2015**, *3*, 22347−22352.
(50) Liu, J.; Chen, L.; Cui, H.; Zhang, J.; Zhang, L.; Su, C.-Y. Applications of metal−organic frameworks in heterogeneous supramolecular catalysis. *Chem. Soc. Rev.* **2014**, *43*, 6011−6061.
(51) Zhu, L.; Liu, X.-Q.; Jiang, H.-L.; Sun, L.-B. Metal−Organic Frameworks for Heterogeneous Basic Catalysis. *Chem. Rev.* **2017**, *117*, 8129−8176.
(52) Shen, L.; Liang, R.; Luo, M.; Jing, F.; Wu, L. Electronic effects of ligand substitution on metal−organic framework photocatalysts: the case study of UiO-66. *Phys. Chem. Chem. Phys.* **2015**, *17*, 117−121.
(53) Hoang, L. T. M.; Ngo, L. H.; Nguyen, H. L.; Nguyen, H. T. H.; Nguyen, C. K.; Nguyen, B. T.; Ton, Q. T.; Nguyen, H. K. D.; Cordova, K. E.; Truong, T. An azobenzene-containing metal−organic framework as an efficient heterogeneous catalyst for direct amidation of benzoic acids: synthesis of bioactive compounds. *Chem. Commun.* **2015**, *51*, 17132−17135.
(54) Doan, T. L. H.; Dao, T. Q.; Tran, H. N.; Tran, P. H.; Le, T. N. An efficient combination of Zr-MOF and microwave irradiation in catalytic Lewis acid Friedel−Crafts benzoylation. *Dalton Trans.* **2016**, *45*, 7875−7880.
(55) Cirujano, F. G.; Corma, A.; Xamena, F. X. L. I. Zirconium-containing metal organic frameworks as solid acid catalysts for the esterification of free fatty acids: Synthesis of biodiesel and other compounds of interest. *Catal. Today* **2015**, *257*, 213−220.
(56) Yang, Y.; Yao, H.-F.; Xi, F.-G.; Gao, E.-Q. Amino-functionalized Zr(IV) metal−organic framework as bifunctional acid−base catalyst for Knoevenagel condensation. *J. Mol. Catal. A: Chem.* **2014**, *390*, 198−205.
(57) Doan, T. L. H.; Dao, T. Q.; Tran, H. N.; Tran, P. H.; Le, T. N. An efficient combination of Zr-MOF and microwave irradiation in catalytic Lewis acid Friedel−Crafts benzoylation. *Dalton Trans.* **2016**, *45*, 7875−7880.
(58) Stock, N.; Biswas, S. Synthesis of Metal-Organic Frameworks-(MOFs): Routes to Various MOF Topologies, Morphologies, and Composites. *Chem. Rev.* **2012**, *112*, 933−969.
(59) Das, A.; Das, S.; Trivedi, V.; Biswas, S. A dual functional MOF-based fluorescent sensor for intracellular phosphate and extracellular 4-nitrobenzaldehyde. *Dalton Trans.* **2019**, *48*, 1332−1343.
(60) Das, A.; Banesh, S.; Trivedi, V.; Biswas, S. Extraordinary sensitivity for $H_2S$ and Fe(III) sensingin aqueous medium by Al-MIL-53-$N_3$ metal−organic framework: in vitro and in vivo applications of $H_2S$ sensing. *DaltonTrans.* **2018**, *47*, 2690−2700.
(61) Das, A.; Anbu, N.; SK, M.; Dhakshinamoorthy, A.; Biswas, S. Highly Active Urea-Functionalized Zr(IV)-UiO-67 Metal−Organic-Framework as Hydrogen Bonding Heterogeneous Catalyst forFriedel−Crafts Alkylation. *Inorg. Chem.* **2019**, *58*, 5163−5172.
(62) Mallakpour, S.; Zadehnazari, A. Molten salt-supported polycondensation of optically active diacid monomers with an aromatic thiazole-bearing diamine using microwave irradiation. *J. Adv. Res.* **2014**, *5*, 311−318.
(63) Cavka, J. H.; Jakobsen, S.; Olsbye, U.; Guillou, N.; Lamberti, C.; Bordiga, S.; Lillerud, K. P. A New Zirconium Inorganic Building Brick Forming Metal Organic Frameworks with Exceptional Stability. *J. Am. Chem. Soc.* **2008**, *130*, 13850−13851.
(64) Valenzano, L.; Civalleri, B.; Chavan, S.; Bordiga, S.; Nilsen, M. H.; Jakobsen, S.; Lillerud, K. P.; Lamberti, C. Disclosing the Complex Structure of UiO-66 Metal Organic Framework: A Synergic Combination of Experiment and Theory. *Chem. Mater.* **2011**, *23*, 1700−1718.
(65) Schaate, A.; Roy, P.; Godt, A.; Lippke, J.; Waltz, F.; Wiebcke, M.; Behrens, P. Modulated Synthesis of Zr-Based Metal−Organic


DOI: 10.1021/acs.inorgchem.9b02608
*Inorg. Chem.* XXXX, XXX, XXX−XXX

Frameworks: From Nano to Single Crystals. *Chem. - Eur. J.* **2011**, *17*, 6643−6651.
(66) Ragon, F.; Campo, B.; Yang, Q.; Martineau, C.; Wiersum, A. D.; Lago, A.; Guillerm, V.; Hemsley, C.; Eubank, J. F.; Vishnuvarthan, M.; Taulelle, F.; Horcajada, P.; Vimont, A.; Llewellyn, P. L.; Daturi, M.; Devautour-Vinot, S.; Maurin, G.; Serre, C.; Devic, T.; Clet, G. Acid-functionalized UiO-66(Zr) MOFs and their evolution after intra-framework cross-linking: structural features and sorption properties. *J. Mater. Chem. A* **2015**, *3*, 3294−3309.
(67) *Accelrys Materials Studio Version 5.0*; Accelrys: San Diego, CA, USA, 2009.
(68) Rappe, A. K.; Casewit, C. J.; Colwell, K. S.; GoddardIII, W. A.; Skiff, W. M. UFF, a full periodic table force field for molecular mechanics and molecular dynamics simulations. *J. Am. Chem. Soc.* **1992**, *114*, 10024−10035.
(69) Howarth, A. J.; Liu, Y.; Li, P.; Li, Z.; Wang, T. C.; Hupp, J. T.; Farha, O. K. Chemical, thermal and mechanical stabilities of metal-organic frameworks. *Nature Rev. Mater.* **2016**, *1*, 1−15.
(70) Nandi, S.; Banesh, S.; Trivedi, V.; Biswas, S. A dinitro-functionalized metal-organic framework featuring visual and fluorogenic sensing of H2S in living cells, human blood plasma and environmental samples. *Analyst* **2018**, *143*, 1482−1491.
(71) Zhou, L.; Zhang, X.; Chen, Y. Modulated synthesis of zirconium metal−organic framework UiO-66with enhanced dichloromethane adsorption capacity. *Mater. Lett.* **2017**, *197*, 167−170.
(72) Pal, S. *Pyridine: A Useful Ligand in Transition Metal Complexes*; IntechOpen: 2018.
(73) Yen, H.-J.; Lin, J.-H.; Su, Y. O.; Liou, G.-S. Observation of ionic hydrogen bonding between anions andtriarylamine-based aromatic polyimides with secondary amine. *Electrochim. Acta* **2018**, *261*, 307−313.
(74) Shivani, P. B.; Chakraborti, A. K. Zinc(II) Perchlorate Hexahydrate Catalyzed Opening of Epoxide Ring by Amines: Applications to Synthesis of (RS)/(R)-Propranolols and (RS)/(R)/(S)-Naftopidils. *J. Org. Chem.* **2007**, *72*, 3713−3722.
(75) Tabatabaeian, K.; Mamaghani, M.; Mahmoodi, N. O.; Khorshidi, A. Solvent-free, ruthenium-catalyzed, regioselective ring-opening of epoxides, an efficient route to various 3-alkylated indoles. *Tetrahedron Lett.* **2008**, *49*, 1450−1454.
(76) Dhakshinamoorthy, A.; Alvaro, M.; Garcia, H. Metal-Organic Frameworks as Efficient Heterogeneous Catalysts for the Regioselective Ring Opening of Epoxides. *Chem. - Eur. J.* **2010**, *16*, 8530−8536.
(77) Placzek, A. T.; Donelson, J. L.; Trivedi, R.; Gibbs, R. A.; De, S. K. Scandium triflate as an efficient and useful catalyst for the synthesis of $\beta$-amino alcohols by regioselective ring opening of epoxides with amines under solvent-free conditions. *Tetrahedron Lett.* **2005**, *46*, 9029−9034.
(78) Luo, R.; Zhang, W.; Zhou, X.; Ji, H. Tannic Acid as a Polyphenol Material-Assisted Synthesis of Cyclic Carbonates Using $CO_2$ as a Feedstock: Kinetic Characteristic and Mechanism Studies. *Chin. J. Chem.* **2017**, *35*, 659−664.



DOI: 10.1021/acs.inorgchem.9b02608
*Inorg. Chem.* XXXX, XXX, XXX−XXX